Carbohydrate Polymers 101 (2014) 240–248

Contents lists available at ScienceDirect

Carbohydrate Polymers

journal homepage: www.elsevier.com/locate/carbpol

The effect of alginate on DNA delivery from layer-by-layer assembled films

Wei-Wen Hu*, Shiang-Lung Tsou

Department of Chemical and Materials Engineering, National Central University, Jhongli City, Taiwan

ARTICLE INFO

Article history:
Received 23 July 2013
Received in revised form 22 August 2013
Accepted 10 September 2013
Available online 19 September 2013

Keywords:
Alginate
Polyelectrolyte multilayer
Layer-by-layer assembly
In situ transfection
Gene delivery

ABSTRACT

Alginate has been previously utilized as an adjuvant in nanoparticle-mediated gene delivery. In this study, we investigated the extent to which alginate promotes *in situ* transfection from polyelectrolyte multilayers (PEMs). After spiking free alginate molecules, DNA release from PEMs was increased and transgene expression was enhanced, suggesting that alginate may compete with DNA to weaken electrostatic interaction within PEMs. Consequently, alginate was applied to compose multilayers with DNA and polyethyleneimine (PEI). Interestingly, the incorporated alginate increased not only deposition but also delivery of DNA from PEMs. Quartz crystal microbalance (QCM) analysis suggested that the deposited alginate enhanced PEI adsorption which in turn augmented subsequent DNA deposition. *In situ* transfection experiments revealed that alginate within PEMs improved not only the level but also the duration of transgene expression. This system should be a potential strategy to regulate gene delivery from scaffolds for tissue engineering application.

1. Introduction

Biomaterials are frequently used as carriers to regulate drug delivery and to sustain the drug effect during the therapeutic period. Layer-by-layer (LbL) assembly is a technique for repeated deposition of charged polymers on material surfaces as polyelectrolyte multilayers (PEMs). Because these PEMs gradually decompose in a physiological environment, this method can be applied for drug delivery (Becker, Johnston, & Caruso, 2010). For gene delivery applications, LbL assembly provides an approach to spatially and temporally control transgene expression so that the transfection can be restricted to target sites. In addition, the duration of delivery should be proportional to the layer number (Jewell & Lynn, 2008). However, the efficiency of DNA delivery highly depends on film stability, and only some of the DNA can be released from PEMs (Blacklock, You, Zhou, Mao, & Oupicky, 2009; Hu et al., 2009). Therefore, a tunable system that can efficiently regulate PEM decomposition to fit the clinical requirement is essential.

Alginate is an anionic polysaccharide frequently used for biomedical applications (Hu & Yu, 2013; Yang et al., 2010). It has been broadly applied in the pharmaceutical area to increase entrapment efficiency and to promote sustained drug release (Liakos et al., 2013; Zheng, Gao, Zhang, & Liang, 2004). Alginate improves gene delivery of polycation-based vectors. Compared with sole administration of cationic polymers as carriers, the addition of alginate during complexation results in excellent transfection efficiency (Douglas, Piecirillo, & Tabrizian, 2006; Patnaik, Arif, Pathak, Singh, & Gupta, 2010). Alginate also reduces cytotoxicity and diminishes unwanted adsorption of serum protein to cationic polyplexes (Lemarchand, Gref, & Couvreur, 2004). Furthermore, anionic alginate competes with DNA; therefore, the electrostatic interaction between DNA and polycations may be weakened (Danielsen, Maurstad, & Stokke, 2005). These studies suggest incorporating alginate into LbL assembly has the potential to regulate PEM stability, and that the released alginate should play a role as an adjuvant to enhance gene delivery.

Therefore, we investigated the level to which alginate promotes DNA release as well as the subsequent *in situ* transfection. Two parts of this study were conducted to support our hypothesis (Fig. 1). Initially, alginate was spiked in the medium before cell seeding on polyethyleneimine (PEI)/DNA multilayer films to determine whether free alginate molecules can loosen multilayered structures to increase gene transfer. After demonstrating the facilitation of suspended alginate for gene delivery of PEMs, we further incorporated alginate into LbL assembly. Alginate was deposited with DNA and PEI to form ternary PEMs. Deposition during PEMs fabrication and the subsequent release were monitored to elucidate the effects of alginate. Finally, *in situ* transfection of NIH/3T3 cells was conducted to evaluate the biocompatibility and transfection efficiency of alginate-incorporated PEMs.

* Corresponding author at: Department of Chemical and Materials Engineering, National Central University, No. 300, Jhongda Rd., Jhongli City, Taoyuan County, Taiwan. Tel.: +886 3 422 7151x34243; fax: +886 3 422 5258.
E-mail address: huweiwen@cc.ncu.edu.tw (W.-W. Hu).

0144-8617/$ – see front matter © 2013 Elsevier Ltd. All rights reserved.
http://dx.doi.org/10.1016/j.carbpol.2013.09.025

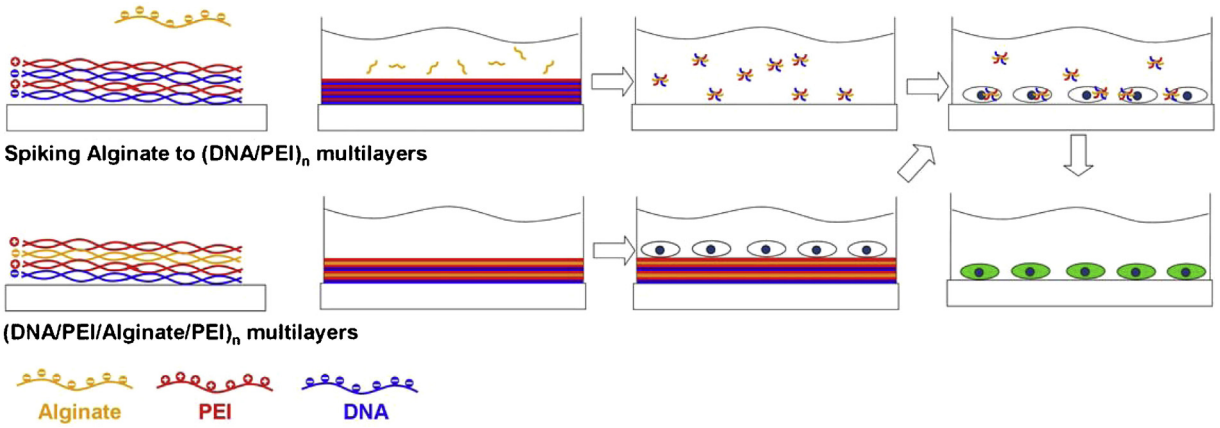

Fig. 1. Two alginate systems to manipulate *in situ* gene delivery on PEMs.

Although alginate has been demonstrated to facilitate polycation gene delivery, the current formula cannot be directly applied to tissue engineering. Compared with conventional polyplex-mediated transfection, PEM-mediated gene delivery has good spatial control and can extend transgene expression. Therefore, the combination of alginate and PEMs should be applicable to *in situ* transfection, and the level and duration of transgene expression may thus be regulated. To the best of our knowledge, this is the first report of using alginate to control gene delivery from PEMs.

2. Materials and methods

2.1. Materials

Sodium alginate (molecular weight of 80–120 kDa) and branched PEI with molecular weights of 25 and 750 kDa were purchased from Sigma–Aldrich (St. Louis, MO, USA). Dulbecco's modified Eagle Medium (DMEM), fetal bovine serum (FBS), and trypsin–EDTA were obtained from Gibco (Carlsbad, CA, USA).

2.2. Plasmid DNA preparation

Plasmid DNA encoding enhanced green fluorescent protein (eGFP) (pEGFP-C3) was purchased from Clontech (Mountain View, CA, USA). The plasmid was cloned and amplified in competent cells *Escherichia coli* DH5α cells (Invitrogen, Carlsbad, CA, USA). The amplified plasmid DNA was isolated with sodium hydroxide and was extracted with phenol and chloroform. Finally, restriction enzyme mapping, polymerase chain reaction (PCR) detection, and DNA sequencing were performed to confirm the quality of the purified plasmid DNA.

2.3. Preparation of PEI, DNA, and Alginate solutions

Polyethyleneimine (molecular weight, 25 kDa) was diluted in phosphate-buffered saline (PBS) to a final concentration of 0.2 g/L, and the final pH was adjusted to 7.4 with 2 N HCl. Sodium alginate was dissolved in PBS to a concentration of 10 g/L, and was further diluted to the required concentrations. The DNA solution was also prepared in PBS at a concentration of 0.25 g/L. All the solutions were filtered through 0.22 μm membranes before the LbL experiments.

2.4. Layer-by-layer assembly of PEMs

Viscous 750 kDa PEI is more appropriate to form stable cationic surfaces than 25 kDa PEI. Therefore, 100 μL of 750 kDa PEI (2 g/L in PBS) was added to 96-well multiplates before LbL assembly. After 2 h of incubation, the PEI solution was removed and the plates were washed thrice with PBS. For DNA/PEI multilayer deposition, the surfaces coated with 750 kDa PEI were successively dipped in DNA and 25 kDa PEI solutions with volumes of 50 μL for each cycle of 20 min and subsequently rinsed thrice with PBS between steps. Similar processes were followed to fabricate DNA/PEI/alginate/PEI multilayers. These cycles were repeated until the desired bilayer or tetralayer number was achieved.

2.5. In situ cell transfection

To evaluate transfer efficiency of PEMs, NIH/3T3 fibroblasts (ATCC, Manassas, VA, USA) were used in this study. These cells (5000 cells/well) were cultured in DMEM supplemented with 10% FBS. In addition, nanoparticles (NPs) formed by DNA and PEI complexation were used as the control group: a 100-μL aliquot of DMEM with 0.5 μg of DNA and 1.25 μg of PEI was added to NIH/3T3 cells seeded in 750 kDa PEI-coated 96-well multiplates 1 day before transfection. The expression of pEGFP-C3 was detected using a fluorescent microscope (Eclipse Ti-U, Nikon, Tokyo, Japan). The cells were washed twice with PBS to remove unwanted debris and impurities. The green channel (Ex. 460–500 nm, Em. 510–560 nm) was used to obtain the results of eGFP, and two different channels (blue: Ex. 330–380 nm, Em. ~420 nm; red: Ex. 510–560 nm, Em. ~590 nm) were applied to confirm the impurities were thoroughly removed from the plate. The green fluorescence of transfected cells was quantified using a fluorescence microplate reader (Synergy H1, Biotek, Winooski, VT, USA) with at an excitation wavelength of 480 nm and an emission wavelength of 511 nm. Relative fluorescent units (RFU) were subtracted from the background and autofluorescence in mock-treated cells.

2.6. Alginate spiking experiments

To determine the effect of alginate molecules on PEM cell transfection, 50 μL of medium with different alginate concentrations was added per well. After 1 h of incubation at 37 °C, NIH/3T3 cells were seeded to determine the improvement in transfection due to the suspended alginate.

2.7. Ultraviolet–visible (UV–Vis) spectrometry

UV–Vis spectrometry (Synergy H1) was performed to monitor DNA within PEMs. The amount of DNA was quantified by

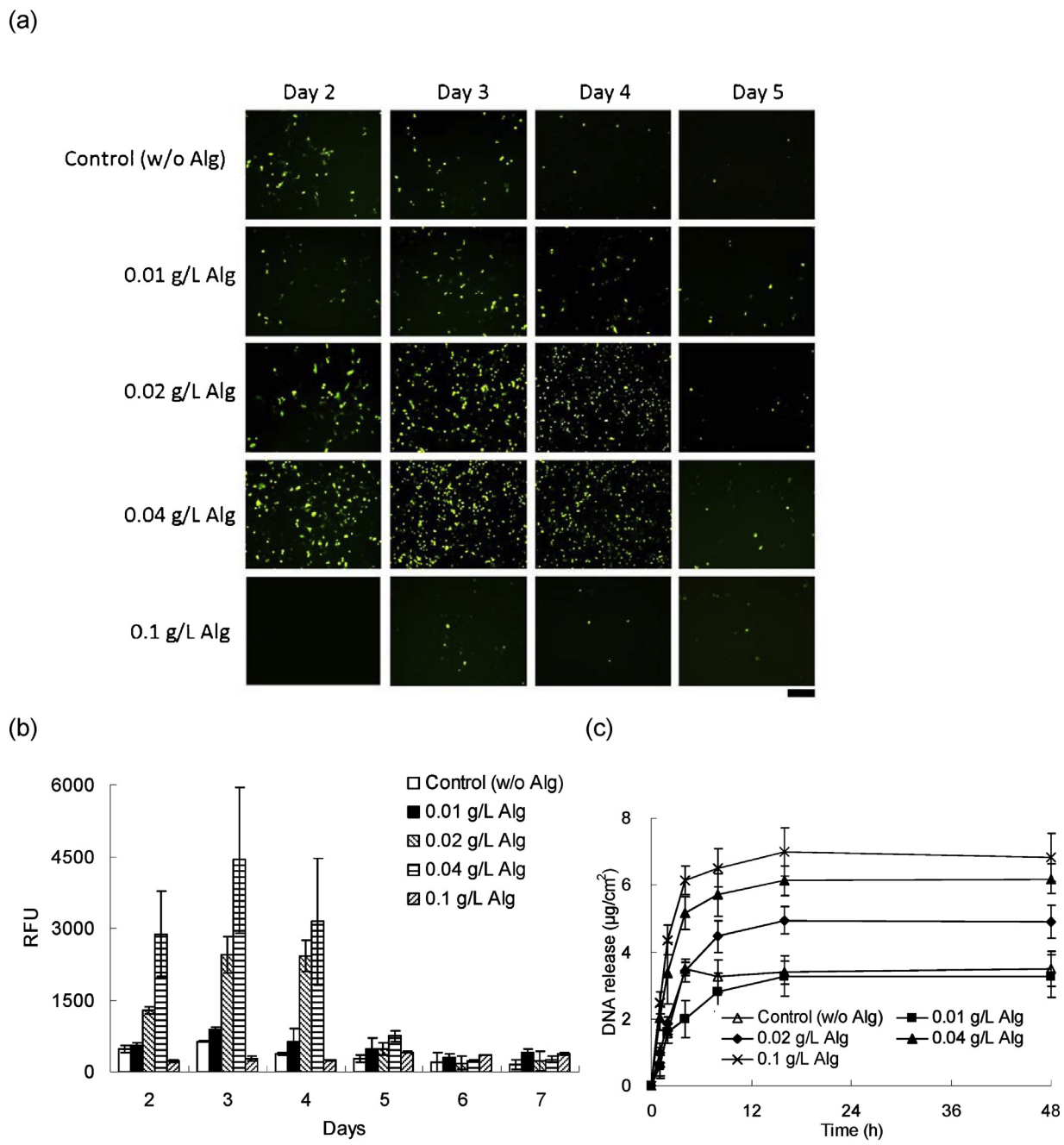

Fig. 2. The effect of spiked alginate on gene delivery from DNA/PEI multilayers. (a) DNA and PEI were deposited as 4 bilayers. Medium with different concentrations of alginate was added to these PEMs for 1 h before seeding the NIH/3T3 cells. The transfected cells were visualized using fluorescent microscopy (scale bar = 200 μm). (b) The expression of eGFP was quantified by fluorescent spectrometry on different days ($n = 3$). (c) Different concentrations of alginate-treated DNA/PEI multilayers were incubated in PBS at 37 °C to simulate their effects on DNA release in an aqueous environment. DNA release was quantified using UV–Vis spectrometry ($n = 3$).

absorbance at 260 nm which is the maximum absorption peak of nucleic base chromophores while PEI and alginate do not exhibit any absorbance. The deposition or release of DNA was normalized by the area of PEMs.

2.8. Fourier transform infrared (FTIR) spectroscopy

The infrared spectrum of PEMs was obtained using attenuated total reflection-Fourier transform infrared (ATR-FTIR) spectroscopy (Spectrum 100, PerkinElmer, Waltham, MA, USA). The IR spectra of alginate, DNA, and PEI were obtained using the KBr pellet method (1 wt.% in KBr).

2.9. Contact angle assessment

The water contact angle of the DNA/PEI/alginate/PEI multilayers was determined using the Drop Shape Analysis system (DSA10, Kruss GmbH, Hamburg, Germany). Four measurements per substrate were taken. Data were presented as the average and standard deviation.

2.10. The compositions of released materials

The fabricated PEMs were incubated in PBS at 37 °C for 48 h to simulate their release into an aqueous environment. The supernatant was analyzed by dynamic light scattering (DLS) analysis

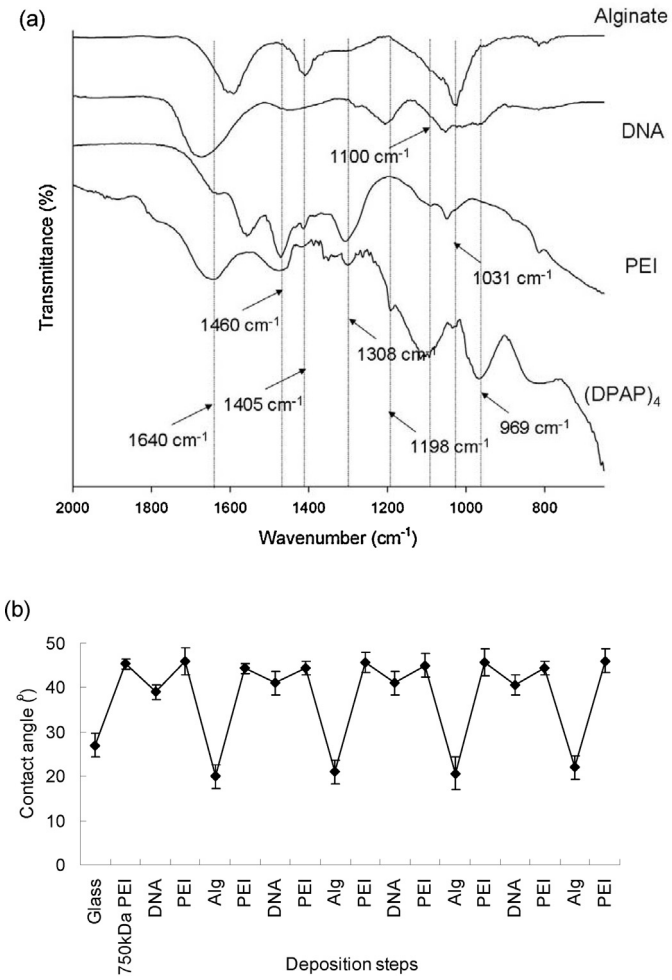

Fig. 3. The characteristics of DNA/PEI/Alginate/PEI polyelectrolyte films. (a) The FT-IR spectra of alginate, DNA, PEI, and $(DPAP)_4$ films. (b) Water contact angle analysis of film surfaces during $(DPAP)_4$ fabrication ($n = 4$)

using a Zetasizer Nano ZS (Malvern, Worcestershire, UK) to determine the properties of the nanoparticles formed by the released components. Size distribution was detected by photon correlation spectroscopy at a 173° scattering angle. Each sample underwent three measurements for reliability conformation, and the mean hydrodynamic diameter was determined by cumulative analysis. Zeta potentials were measured by laser Doppler anemometry in samples that were placed in disposable capillary cells to evaluate the surface charges of the nanoparticles according to their electrophoretic mobility.

A gel retardation assay was applied to examine free DNA in the supernatant and to determine the complexation efficiency of released material. Samples were loaded on a 1% agarose gel to perform electrophoresis at 100 V for 40 min and were stained with ethidium bromide.

2.11. Quartz crystal microbalance (QCM) analysis

Piezoelectric quartz crystals, consisting of a 9 MHz AT cut quartz slab with a layer of gold electrode on each side, were obtained from ANT Technology (Taipei, Taiwan). Frequency variation was recorded by the Affinity Detection system (ANT, Taipei, Taiwan). The area of the quartz was 0.091 cm^2, and the oscillatory frequency change (ΔF) corresponds to a mass change of 0.391 ng/Hz.

Quartz chips were cleaned with sulfuric acid and hydrogen peroxide and were then thoroughly rinsed with double distilled H_2O (ddH_2O) and subsequently air-dried. Polyethyleneimine solution with a molecular weight of 750 kDa (0.1 g/L) was coated onto QCM chip surfaces in a volume of 50 μL and incubated at 37 °C overnight. The chips were thoroughly rinsed with ddH_2O before measurement. The flow rate was 90 μL/min throughout the experiment, and PBS was applied to flush the chips between deposition steps until frequency equilibrium was achieved.

2.12. Biocompatibility of PEMs

To evaluate biocompatibility of PEMs, NIH/3T3 cells were seeded on their surfaces, and 3-(4,5-dimethylthiazol-2-yl)-5-(3-carboxymethoxyphenyl)-2-(4- sulfophenyl)-2H-tetrazolium (MTS) assays were performed to quantify cell viability at days 3 and 5 according to the manufacturer's instructions. In brief, CellTiter 96 AQueous kit (Promega, Madison, WI, USA) were used 20 μL/well and required 1 h of incubated at 37 °C. The samples were transferred to 96-well multiplates and read at a wavelength of 490 nm. The results were normalized by those obtained for cells cultured on normal tissue culture polystyrene (TCPS) surfaces.

3. Results and discussion

3.1. Alginate in medium promotes gene delivery from polyelectrolyte multilayer (PEM)

Because alginate has been demonstrated to promote transfection when added during polyplex formation (Patnaik et al., 2010), it should potentially facilitate *in situ* transfection on PEMs. Therefore, a spiking experiment was conducted initially to prove our hypothesis. Different concentrations of alginate were incubated on PEI/DNA multilayers for 1 h before cell seeding. The expression efficiency of eGFP was highly correlated with the spiked alginate concentration, which increased with increasing of alginate concentration; however, green fluorescence was diminished when the alginate concentration rose to 0.1 g/L (Fig. 2a and b). The release of DNA was analyzed using UV–Vis spectrometry (Fig. 2c). Almost no difference was observed between the control group and the group spiked with 0.01 g/L of alginate. However, for alginate concentrations higher than 0.01 g/L, DNA release increased with increasing of alginate concentrations, suggesting that alginate competed with DNA to loosen the structure of the multilayer, which induced more DNA to be released into solution for transfection.

A similar study was performed by Kharlampieva's group in which the release of dye embedded in LbL assembled films was triggered by the presence of oppositely charged polyelectrolyte due to competitive complexation (Kharlampieva & Sukhishvili, 2004). In the present study, the anionic alginate may have complexed with the cationic PEI in the multilayer, which further weakened the interaction between PEI and DNA within the multilayer and eventually enhanced DNA delivery from PEMs. Because spiked anionic alginate may attract released PEI to further complex with DNA to form ternary nanoparticles, the composition of these polyplexes plays an important role in transfection (Douglas & Tabrizian, 2005). Patnaik et al. complexed different concentrations of alginate with PEI and DNA, and their results suggest that transfection efficiency is highly affected by nanoparticle composition because only polyplexes with appropriate alginate ratios promote gene delivery (Patnaik et al., 2010). Because anionic alginate may compete with DNA for complexing with PEI, the interaction between DNA and PEI can be modulated so that DNA dissociation from nanoparticles within endosomes is promoted (Jiang, Min, Oh, & Hahn, 2007). However, too much of alginate probably reduced the efficiency of DNA complexation; therefore, the group spiked with 0.1 g/L alginate demonstrated poor transfection results (Patnaik et al., 2006).

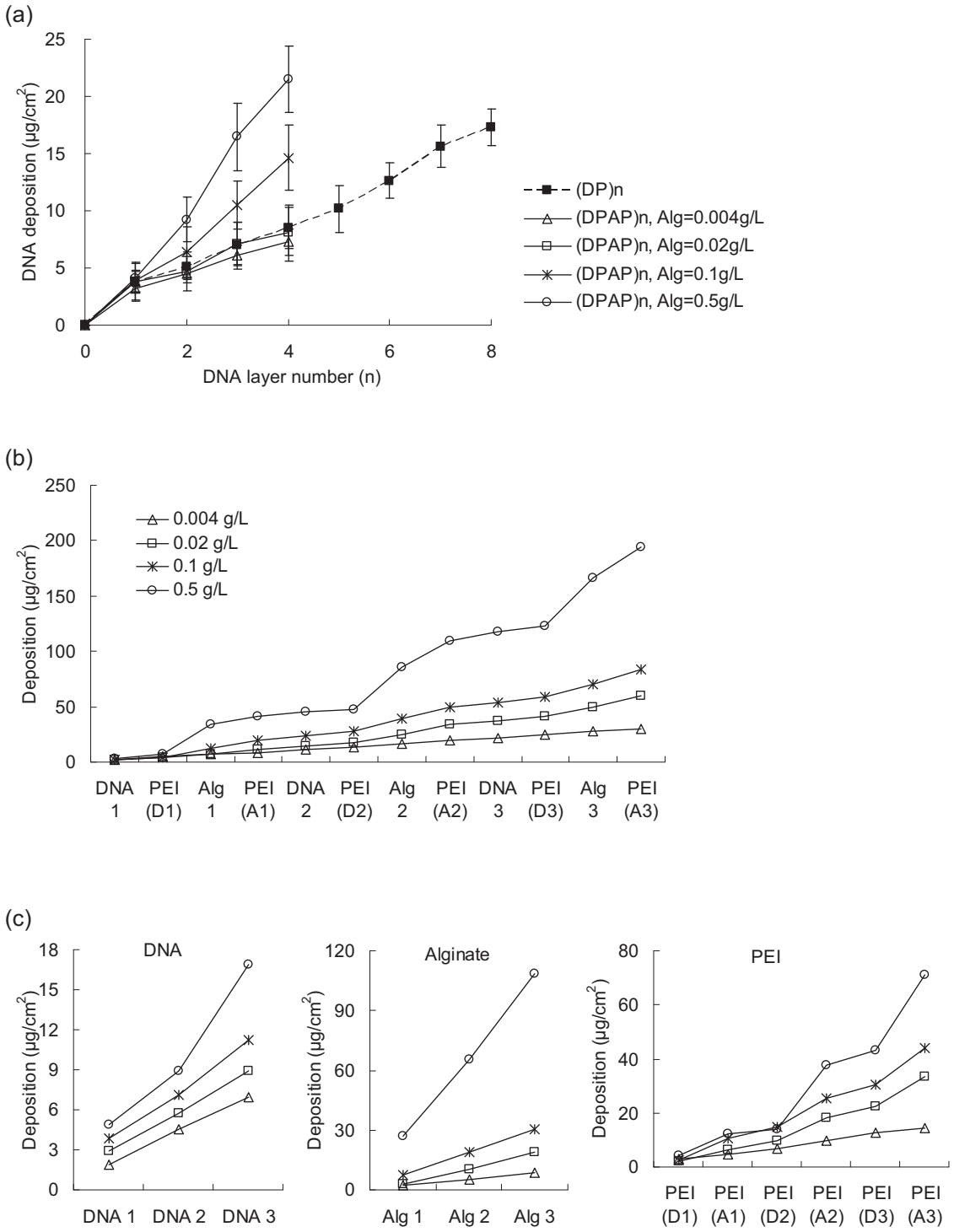

Fig. 4. Deposition of DNA on $(DPAP)_4$ films. (a) Different concentrations of alginate were applied to deposit $(DPAP)_4$ films. The DNA deposited in PEMs was analyzed by UV–Vis spectrometry ($n = 3$). (b) Similarly, QCM analysis was also applied to monitor the mass change on quartz chips during LbL assembly. (c) To elucidate the effect of alginate on increasing DNA deposition, the cumulative QCM results of deposited DNA, alginate, and PEI were individually compared at different tetralayer numbers.

3.2. Incorporation of alginate into PEMs

Although spiked alginate promoted the *in situ* transfection on the multilayers, this method cannot be directly applied to a clinical situation. Incorporating alginate into PEMs is an approach available for tissue engineering. Therefore, we developed a ternary PEM fabrication such that PEMs were assembled in the order of DNA–PEI–alginate–PEI, $(DPAP)_n$, and the steps were repeated until the desired number of tetralayers was achieved.

To analyze the chemical properties of the deposited films, ATR-FTIR was performed. Alginate, DNA, and PEI demonstrated specific peaks in their IR spectra (Fig. 3a). Alginate had two characteristic peaks at 1405 and 1031 cm^{-1}, which were attributed to its C—O stretching and asymmetric absorption of COO^-, respectively (Yu & Fan, 2008; Zhu, Ji, & Shen, 2004). Two specific peaks of DNA were observed at 1198 and 969 cm^{-1}, which were ascribed to the phosphate groups and the —C—C— groups of deoxyribose, respectively (Malins et al., 2005). For PEI, the peaks at 1640 and 1308 cm^{-1} were

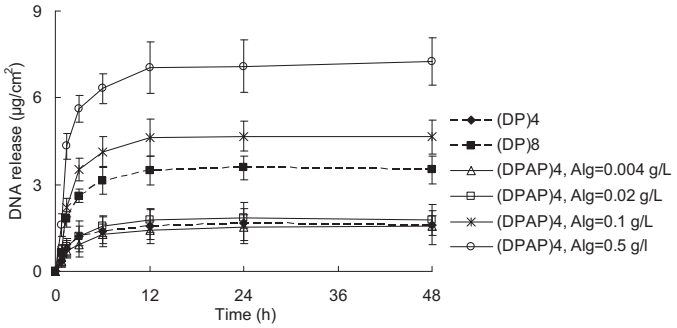

Fig. 5. The release of DNA from $(DPAP)_4$ films. The deposited $(DPAP)_4$ films were immersed in PBS at 37 °C to simulate DNA release in an aqueous environment. The released DNA was sampled at different time points and was quantified by UV–Vis spectrometry ($n = 3$).

due to the scissoring vibration of primary amines and the stretching vibration of C—N bonds, respectively (Hong, Lee, Kim, Chung, & Choi, 2009). Absorptions at 1100 and 1460 cm^{-1} in the PEI spectrum was due to the bending vibration of N—H and CH_2 bonds, respectively (Veerakumar, Velayudham, Lu, & Rajagopal, 2012). The multilayered $(DPAP)_n$ films demonstrated all these characteristic peaks, indicating that PEI, DNA, and alginate were successfully deposited by LbL assembly.

Water contact angle analysis was performed to investigate the changes in surface properties with deposition processes. The contact angles varied with the steps of LbL assembly (Fig. 3b). Because the hydrophobicity of the surface alternatively changed with the highest layer, the deposited DNA, PEI, and alginate were assembled on the material surfaces in a layered manner.

3.3. Deposition of DNA in PEMs

As alginate layers were incorporated into the $(DPAP)_n$ films, we further determined the effect of alginate on DNA loading efficiency. The amount of DNA within PEMs was determined using a UV–Vis spectrometer (Fig. 4a). Deposition of DNA was regulated by varying the alginate concentration from 0.004 to 0.5 g/L during the LbL process. The 0.004 and 0.02 g/L groups exhibited DNA adsorption similar to that of the control group of DNA/PEI multilayer, $(DP)_n$. However, DNA deposition improved significantly when the concentration was increased to 0.1 g/L. Furthermore, the 0.5 g/L group demonstrated the highest DNA adsorption; thus, 4 layers of DNA in the $(DPAP)_4$ films were more effective than 8 layers of DNA in the control group $(DP)_8$ films.

QCM analysis was applied to monitor the mass change during LbL assembly and to investigate the mechanism of enhanced DNA deposition by the alginate layers. Increasing the alginate concentration highly enhanced deposition efficiency of $(DPAP)_n$ film (Fig. 4b). The accumulative masses of deposited DNA, alginate, and PEI were individually analyzed to elucidate the improvement mechanism of alginate (Fig. 4c). Similar to the results of UV–Vis spectrometry, the immobilized DNA was enhanced by incorporating alginate. Alginate adsorption increased with increasing alginate concentration. Interestingly, the adsorption of PEI highly depended on the anionic layer. Compared with PEI adsorption on the top of DNA [PEI (D1), PEI (D2), PEI (D3)], the deposition of PEI was significantly improved when alginate was the uppermost layer [PEI (A1), PEI (A2), PEI (A3)].

In contrast to DNA, the adsorption of alginate was relatively high, probably because the charge density of alginate was lower than that of DNA; therefore, large amounts of alginate molecules were required to achieve equilibrium (Song et al., 2009). When PEI was added to the top of alginate, more alginate attracted more PEI deposition. In addition, low-charged alginate molecules may exist

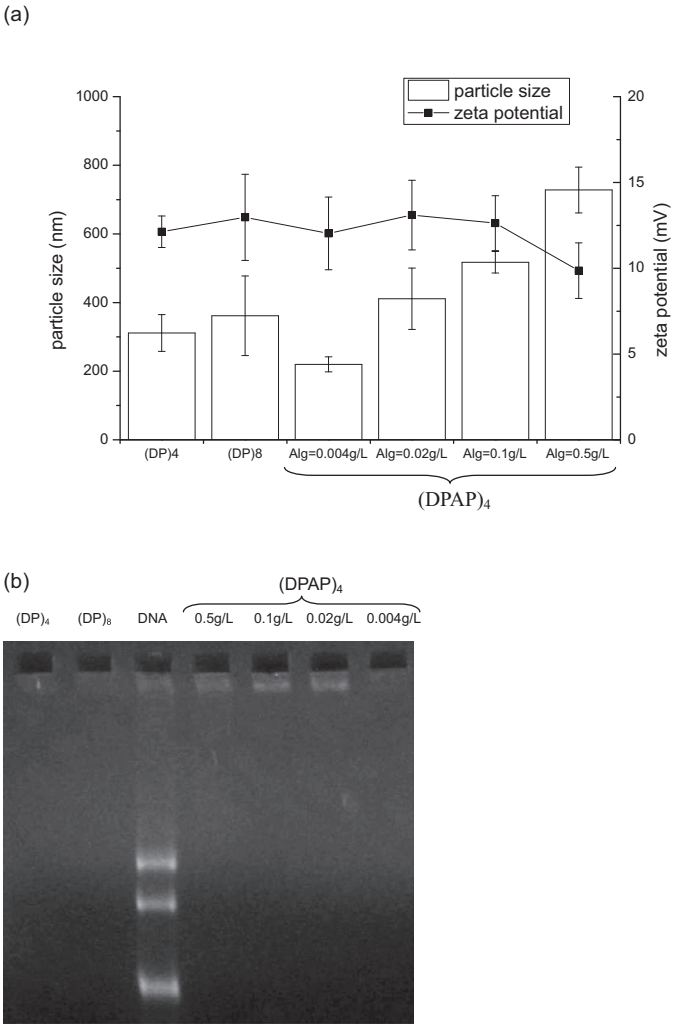

Fig. 6. Properties of materials released from $(DPAP)_4$ films. After incubating the PEMs in PBS at 37 °C for 48 h, the supernatants were collected. (a) Sizes and zeta potentials of the nanoparticles were evaluated by DLS analysis ($n = 3$). (b) DNA loading efficiencies of complexed nanoparticles were analyzed by electrophoresis analysis.

in a random-coiled form; therefore, the alginate layers were not compact. Such a loose structure could promote the interdiffusion of PEI into the alginate layer during LbL assembly, which increased PEI adsorption (Zacharia, Modestino, & Hammond, 2007). Because PEI adsorption was enhanced on the alginate layer, the next step of

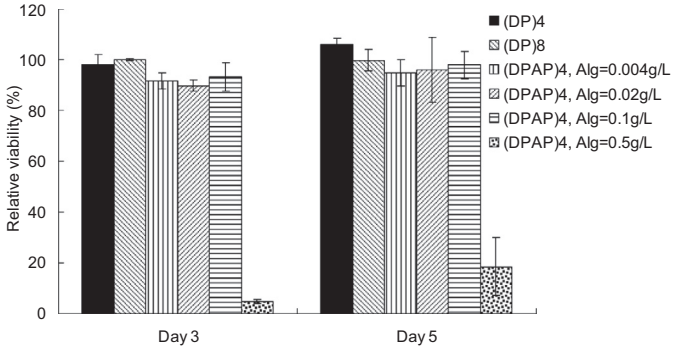

Fig. 7. Biocompatibility of the PEMs. NIH/3T3 cells were cultured on PEMs for 3 and 5 days. The viabilities of surface cells were determined by the MTS assay. The spectrometric results were normalized by the results of cells grown on TCPS surfaces ($n = 3$).

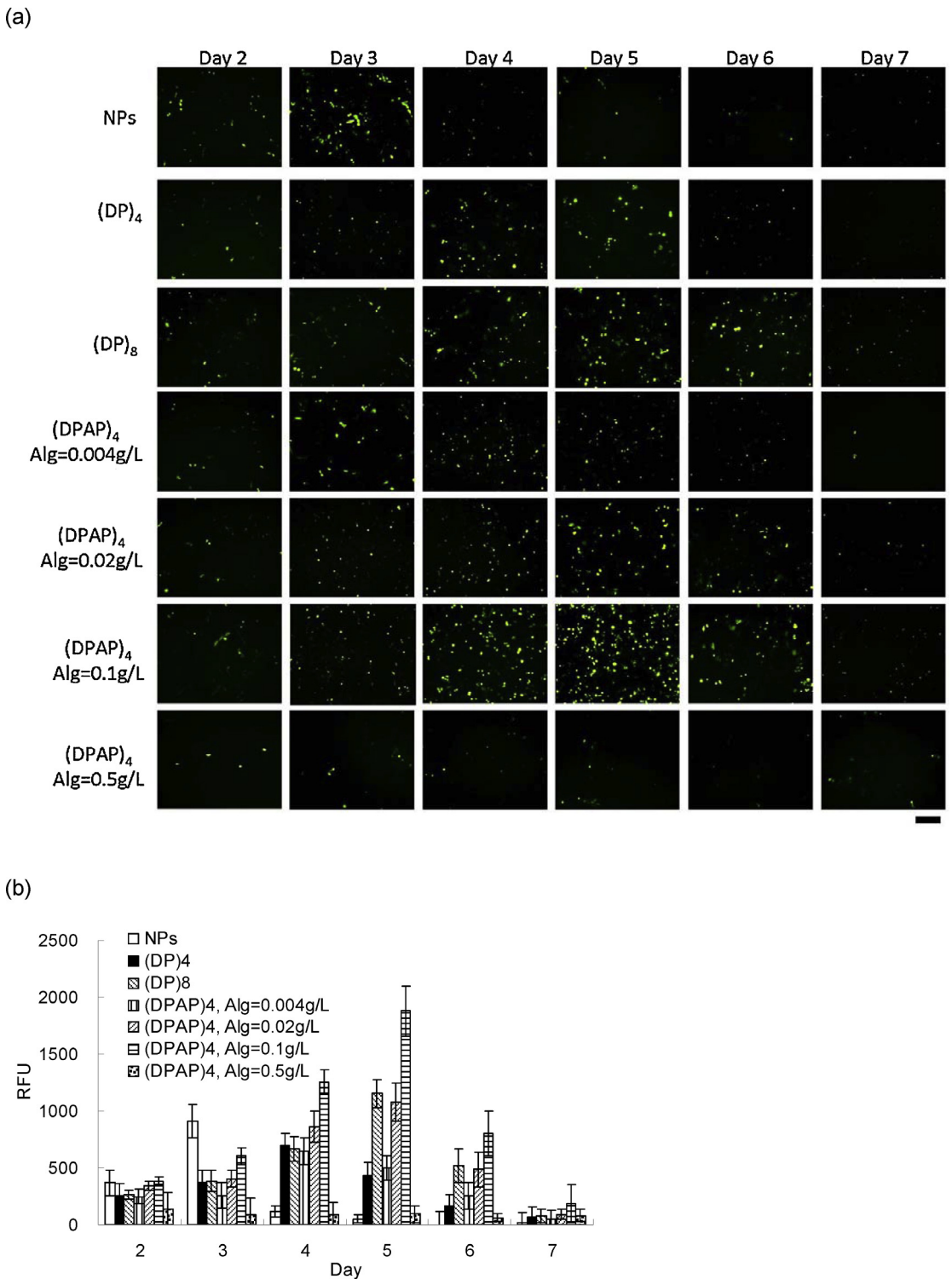

Fig. 8. *In situ* transfection of cells on PEMs. Different concentrations of alginate were applied to deposit the $(DPAP)_4$ films, and NIH/3T3 cells were cultured on these surfaces for *in situ* transfection. Nanoparticles (NPs) formed by PEI/DNA complexation were also applied to transfect cells as the control group. (a) eGFP expressing cells were visualized by fluorescent microscopy (scale bar = 200 μm). (b) eGFP expression was quantified by the fluorescent spectrometry ($n = 3$).

DNA deposition increased, which in turn promoted the deposition of the subsequent layers. Therefore, the application of alginate can augment the deposition efficiency of PEMs.

3.4. Release of DNA from PEMs

After 4 tetralayer deposition, the films were incubated in PBS at 37 °C to simulate release into the aqueous environment (Fig. 5). The release profiles of DNA from PEMs fabricated with 0.004 or 0.02 g/L alginate were similar to that of the $(DP)_4$ films. In contrast, DNA delivery of the 0.1 g/L group was higher than that of the $(DP)_8$ film. The 0.5 g/L group demonstrated the highest delivery efficiency, which was twofold and fourfold that of the $(DP)_8$ and $(DP)_4$ films, respectively. These results suggest that the incorporation of alginate improved not only immobilization but also DNA release from PEMs. A reason for this could be that the degradation of

alginate promoted the decomposition of PEMs (Bajpai & Tankhiwale, 2006).

Because the released DNA and alginate may complex with PEI, the nanoparticles that were formed were examined by DLS. No significant trend in surface charge was observed and the zeta potentials of all the groups were between 10 and 13 mV (Fig. 6a). However, the sizes of particles released from the $(DPAP)_4$ films increased with increasing alginate concentration during LbL assembly, suggesting that the alginate layers in PEMs were critical to determine the composition of the nanoparticles. The diameters of the nanoparticles were less than 500 nm, except those in the 0.5 g/L group, and were suitable for cell uptake (Wang, Zhou, Ma, Li, & Gu, 2009). The supernatants were also analyzed by electrophoresis to investigate complexation efficiency (Fig. 6b). Similar to the $(DP)_4$ and $(DP)_8$ films, no free DNA was detected in the release solution of $(DPAP)_4$ films using 0.004 g/L alginate. When the alginate concentration was increased to ≧0.02 g/L, slight bands were observed below the wells because alginate competed with DNA for complexation with PEI; thus, DNA within polyplexes may move slightly in the electric field. Nevertheless, free DNA was still unavailable. These results suggest that alginate may mediate the interaction between DNA and PEI; however, the complexation efficiency did not decrease significantly.

3.5. *In situ* cell transfection and PEM biocompatibility

To evaluate whether alginate incorporated into PEMs promotes cell transfection, NIH/3T3 cells were seeded on PEMs. Plasmid DNA encoding eGFP was used as a reporter gene for the *in vitro* study, and the intensity of green fluorescence was quantified by fluorescent spectrometry to determine transgene expression efficiency. Before the transfection experiment, the MTS assay was performed at days 3 and 5 to analyze the viability of cultured cells on PEMs (Fig. 7). All the PEMs maintained the viability of surface cells except $(DPAP)_4$ films that used 0.5 g/L alginate during fabrication. The low viability of the 0.5 g/L group was due to the cytotoxicity of PEI because the deposition of PEI was highly enhanced by the alginate layers (Fig. 4c).

The expression of eGFP by cells on $(DPAP)_4$ films fabricated with 0.004 g/L of alginate was similar to that of the $(DP)_4$ films, which was consistent with their deposition and release results (Fig. 8). Alginate deposition promoted *in situ* transfection; the 0.02 g/L group had similar performance to the $(DP)_8$, and the performance of the 0.1 g/L group was twofold and fourfold of the $(DP)_8$ and $(DP)_4$ films, respectively. These results suggest that alginate enhanced DNA immobilization and release from the PEMs. It was interesting that the 0.02 g/L group had higher expression efficiency than the $(DP)_4$ films, although there were almost no differences in the deposition and release results between these two groups (Fig. 5). This result suggests that the released alginate likely enhanced gene delivery. However, when the alginate concentration was increased to 0.5 g/L, the fabricated $(DPAP)_4$ film was not suitable for gene delivery because green fluorescence was almost undetectable, which may have been due to its low bioactivity (Fig. 7).

Compared with the transfection of DNA/PEI complexed nanoparticles (NPs), PEMs sustained transgene expression. Cells transfected with the NPs expressed the highest GFP on day 3. In contrast, transfection of the $(DP)_4$ film and the $(DPAP)_4$ film fabricated with 0.004 g/L alginate had the highest GFP expression on day 4. When alginate was increased to 0.02 and 0.1 g/L, the fabricated $(DPAP)_4$ films showed the highest GFP expression on Day 5, which were similar to that of the DNA/PEI multilayers with a high bilayer number, *i.e.* $(DP)_8$ films. Take together, these results suggest that the incorporation of alginate into PEMs not only improved transfection but also extended the expression duration of the transgene.

4. Conclusion

Anionic alginate promoted gene delivery from LbL assembled PEMs. Because alginate interacts with polycations through electrostatic forces, it modulates the complexation between DNA and nonviral vectors. By spiking alginate in the medium, DNA release was increased and transgene expression was improved. The multilayer films composed of $(DPAP)_n$ demonstrated that the alginate layers facilitated the adsorption of PEI, which enhanced DNA adsorption. In addition, the released alginate augmented transfection. These results indicate that alginate could be used to improve the *in situ* transfection of PEMs.

Acknowledgements

This research was supported by the grant of NSC 99-2221-E-008-007-MY2 from the National Science Council of Taiwan, and 101CGH-NCU-A2 from the National Central University and Cathy General Hospital Joint Research Center.

References

Bajpai, S. K., & Tankhiwale, R. (2006). Investigation of water uptake behavior and stability of calcium alginate/chitosan bi-polymeric beads: Part-1. *Reactive and Functional Polymers*, *66*(6), 645–658.

Becker, A. L., Johnston, A. P. R., & Caruso, F. (2010). Layer-by-layer-assembled capsules and films for therapeutic delivery. *Small*, *6*(17), 1836–1852.

Blacklock, J., You, Y. Z., Zhou, Q. H., Mao, G. Z., & Oupicky, D. (2009). Gene delivery in vitro and in vivo from bioreducible multilayered polyelectrolyte films of plasmid DNA. *Biomaterials*, *30*(5), 939–950.

Danielsen, S., Maurstad, G., & Stokke, B. T. (2005). DNA–polycation complexation and polyplex stability in the presence of competing polyanions. *Biopolymers*, *77*(2), 86–97.

Douglas, K. L., & Tabrizian, M. (2005). Effect of experimental parameters on the formation of alginate-chitosan nanoparticles and evaluation of their potential application as DNA carrier. *Journal of Biomaterials Science – Polymer Edition*, *16*(1), 43–56.

Douglas, K. L., Piecirillo, C. A., & Tabrizian, M. (2006). Effects of alginate inclusion on the vector properties of chitosan-based nanoparticles. *Journal of Controlled Release*, *115*(3), 354–361.

Hong, H., Lee, S., Kim, T., Chung, M., & Choi, C. (2009). Surface modification of the polyethyleneimine layer on silicone oxide film via UV radiation. *Applied Surface Science*, *255*(12), 6103–6106.

Hu, W. W., & Yu, H. N. (2013). Coelectrospinning of chitosan/alginate fibers by dual-jet system for modulating material surfaces. *Carbohydrate Polymers*, *95*(2), 716–727.

Hu, Y., Cai, K. Y., Luo, Z., Zhang, R., Yang, L., Deng, L. H., et al. (2009). Surface mediated in situ differentiation of mesenchymal stem cells on gene-functionalized titanium films fabricated by layer-by-layer technique. *Biomaterials*, *30*(21), 3626–3635.

Jewell, C. M., & Lynn, D. M. (2008). Multilayered polyelectrolyte assemblies as platforms for the delivery of DNA and other nucleic acid-based therapeutics. *Advanced Drug Delivery Reviews*, *60*(9), 979–999.

Jiang, G., Min, S. H., Oh, E. J., & Hahn, S. K. (2007). DNA/PEI/Alginate polyplex as an efficient in vivo gene delivery system. *Biotechnology and Bioprocess Engineering*, *12*(6), 684–689.

Kharlampieva, E., & Sukhishvili, S. A. (2004). Release of a dye from hydrogen-bonded and electrostatically assembled polymer films triggered by adsorption of a polyelectrolyte. *Langmuir*, *20*(22), 9677–9685.

Lemarchand, C., Gref, R., & Couvreur, P. (2004). Polysaccharide-decorated nanoparticles. *European Journal of Pharmaceutics and Biopharmaceutics*, *58*(2), 327–341.

Liakos, I., Rizzello, L., Bayer, I. S., Pompa, P. P., Cingolani, R., & Athanassiou, A. (2013). Controlled antiseptic release by alginate polymer films and beads. *Carbohydrate Polymers*, *92*(1), 176–183.

Malins, D. C., Gilman, N. K., Green, V. M., Wheeler, T. M., Barker, E. A., & Anderson, K. M. (2005). A cancer DNA phenotype in healthy prostates, conserved in tumors and adjacent normal cells, implies a relationship to carcinogenesis. *Proceedings of the National Academy of Sciences of the United States of America*, *102*(52), 19093–19096.

Patnaik, S., Aggarwal, A., Nimesh, S., Goel, A., Ganguli, M., Saini, N., et al. (2006). PEI-alginate nanocomposites as efficient in vitro gene transfection agents. *Journal of Controlled Release*, *114*(3), 398–409.

Patnaik, S., Arif, M., Pathak, A., Singh, N., & Gupta, K. C. (2010). PEI-alginate nanocomposites: Efficient non-viral vectors for nucleic acids. *International Journal of Pharmaceutics*, *385*(1-2), 194–202.

Song, Z. J., Yin, J. B., Luo, K., Zheng, Y. Z., Yang, Y., Li, Q., et al. (2009). Layer-by-layer buildup of poly(L-glutamic acid)/chitosan film for biologically active coating. *Macromolecular Bioscience*, *9*(3), 268–278.

Veerakumar, P., Velayudham, M., Lu, K. L., & Rajagopal, S. (2012). Polyelectrolyte encapsulated gold nanoparticles as efficient active catalyst for reduction of nitro compounds by kinetic method. *Applied Catalysis A: General*, *439*, 197–205.

Wang, X. L., Zhou, L. Z., Ma, Y. J., Li, X., & Gu, H. C. (2009). Control of aggregate size of polyethyleneimine-coated magnetic nanoparticles for magnetofection. *Nano Research*, *2*(5), 365–372.

Yang, S. J., Chang, S. M., Tsai, K. C., Chen, W. S., Lin, F. H., & Shieh, M. J. (2010). Effect of chitosan-alginate nanoparticles and ultrasound on the efficiency of gene transfection of human cancer cells. *Journal of Gene Medicine*, *12*(2), 168–179.

Yu, G. H., & Fan, Y. B. (2008). Preparation of poly(D,L-lactic acid) scaffolds using alginate particles. *Journal of Biomaterials Science – Polymer Edition*, *19*(1), 87–98.

Zacharia, N. S., Modestino, M., & Hammond, P. T. (2007). Factors influencing the interdiffusion of weak polycations in multilayers. *Macromolecules*, *40*(26), 9523–9528.

Zheng, C. H., Gao, J. Q., Zhang, Y. P., & Liang, W. Q. (2004). A protein delivery system: biodegradable alginate-chitosan-poly(lactic-co-glycolic acid) composite microspheres. *Biochemical and Biophysical Research Communications*, *323*(4), 1321–1327.

Zhu, H., Ji, J., & Shen, J. (2004). Construction of multilayer coating onto poly-(DL-lactide) to promote cytocompatibility. *Biomaterials*, *25*(1), 109–117.